Creating of Digital Surface Model and Orthophoto from ASTER Satellite Data and their Application in Land/Water Research

Dana TOLLINGEROVÁ[1] and Karel PAVELKA[2]

[1]Faculty of Environmental Science, Czech University of Life Sciences in Prague, Prague, Czech Republic; [2]Faculty of Civil Engineering, Czech Technical University in Prague, Prague, Czech Republic

Abstract: Satellite data has become a commonly used information source. Landscapes components such as water, inorganic substances, vegetation, and the atmosphere may be distinguished making use of their spectral characteristics. The above mentioned components may be further divided. For example, inorganic substances may be subdivided into soil, minerals, build up areas etc. The spectral characteristics of soils are determined by moisture, humus contents, mineral composition, surface structure, and the stage of eroding processes. The development in remote sensing tends either to the data acquisition in more spectral bands or the improvement of the resolution of remote sensing data. The terra satellite ranks among new generation satellites; its orbital parameters are similar to the parameters of the Landsat system. ASTER (Advanced Spaceborn Thermal Emission and Reflection Radiometer) is one of the onboard instruments on Terra satellite and captures data in 14 spectral bands. The VNIR (Visible Near Infrared) subsystem provides 15 m spatial resolution data. Two of the VNIR subsystem telescopes enable stereoscopic data evaluation. A stereo-pair consists of 3N (nadir) and 3B (backward) images. A couple of 3N and 3B images can be used for the creation of a digital surface model (DSM) and orthophoto. This article describes the creation of DSM and orthophoto of an area located in the north-west part of the Czech Republic. Images of the area were made in years 2002 and 2005. In this work, level 1B images were used, i.e. images with radiometric and geometric corrections already applied. The model was created through the use of 21 control points selected in each scene. The standard error of co-ordinates of the control points is up to 15 m, the elevation standard error is approx. 30 m. The accuracy of the final DSM and orthophoto was tested on a set of 13 check points. The position standard error in DSM and orthophoto is approx. 15 m, i.e. just about the size of one pixel of the original data. The elevation standard error of the checkpoints is up to 40 m. The output can be used as a basis for small-scale maps. Using one scene acquired by ASTER instruments, a DSM and orthophoto covering an area of 60 × 60 km can be created.

Keywords: remote sensing; ASTER; digital surface model; orthophoto

Digital processing ranks among the contemporary data processing technologies. One of the commonly used information sources is remote sensing (RS). The technology of RS was used for the first time in the thirties of the last century. It has been implemented on a large scale in the sixties. Already in the eighties, RS was used for determining data concerning soil moisture. RS data

Supported by the the Ministry of the Environment of the Czech Republic, Project No. VaV-SM/10/70 04.

are used in geographic information systems as an information source used for monitoring the surface changes in time and position. Instruments placed on Earth artificial satellites enable environmental monitoring, so it is also possible to acquire the information necessary for understanding the processes and phenomena on the land surface. The Earth Observing System (EOS) is a multinational and multi-disciplinary mission focused on the understanding of the Earth environment and its components. At the present time, a new similar project called Global Monitoring for Environment and Security has been started within the European Union.

The EOS project focuses on scientific areas such as:

– Biology and biochemistry of ecosystems as well as carbon cycles
– Circulation of water and energy
– Climate variations and forecasting
– Chemistry of the atmosphere
– Research in the earth core

A sufficient volume of the collected data will enable to forecast diverse processes related to the Earth, i.e.:

– Hydrological
– Biochemical
– Atmospheric
– Ecological
– Geophysical

One of the satellites used in the EOS programme is the Terra satellite (its original name is EOS AM-1 – Earth Observing System Ante Meridian). The Terra is a three-axe satellite that circles in a polar sun-synchronous orbit. Its ground track repeat cycle is 16 days. Spatial resolution of the data is 15–90–1000 m and a swath width is 60–2330 km. The data are acquired by passive instruments which sense the reflected and emitted radiation. The satellite carries these instruments (Anonym 2006b, c):

– CERES (Clouds and Earth Radiant Energy System) – a broadband scanning radiometer with bolometers, used for monitoring the Earth radiation balance. Captured data help forecast weather more precisely

– MISR (Multi-angle Imaging Spectro-Radiometer) – a 4-channel scanning radiometer with cameras pointed at nine different angles. It investigates the reflectance of the atmosphere, clouds, and land surface, especially the vegetation cover

– MODIS (Moderate Resolution Imaging Spectro-Radiometer) – a 36-channel scanning radiometer with moderate resolution is useful in the studies of physical and biological processes occurring in the oceans and on land surface

– MOPITT (Measurements of Pollution in the Troposphere) – a spectrometer permitting studies of the lower atmosphere, it is designed especially to monitor the pollution caused by carbon monoxide and methane

– ASTER (Advanced Spaceborn Thermal Emission and Reflection Radiometer) is a 14-channel high resolution imaging radiometer which measures cloud properties, vegetation index, surface mineralogy, soil properties, surface temperature, and surface topography. It is also used for monitoring natural disasters; it has three detection subsystems:

(1) Visible Near Infrared (VNIR) – this subsystem works in visible and near infrared bands, it has an adjustable swath width ± 24 degrees; two telescopes (a nadir looking and a backwards looking one) enable a stereoscopic reconstruction

(2) Short-wave Infrared (SWIR) – captures mid-infrared data (in 6 channels)

(3) Thermal Infrared (TIR) – captures thermal infrared data (in 5 channels)

The data collected by means of the ASTER technology may be used in the assessment of spectral properties of the biosphere, hydrosphere, lithosphere, and atmosphere. With its spectral range of 0.52 μm–11.65 μm, the ASTER technology closely resembles the properties of the ETM+ scanner (Enhanced Thematic Mapper) carried on board of the Landsat 7 satellite. The ETM+ scans in 8 zones in the range of 0.45 μm–12.50 μm with space resolution in channels 1–6 – 30 m, 7 (thermal) – 60 m, 8 (panchromatic) – 15 m.

It can be assumed that the data collected by ASTER may serve a similar purpose as that collected by EMT+. High spectral resolution also allows a work similar to the hyperspectral data analysis. The standard image classification can be replaced with the help of spectral libraries mapping. Furthermore, it is possible, with the help of the data collected, to perform thematic surface mapping including the vegetation cover, polar glaciation, or cloud formation. The collected data allows monitoring natural disasters such as floods, volcanic activities, fires etc. Channels 3N and 3B may be coupled for stereo reception and the data can serve for the calculation of a digital model or ortophotos creation.

The spectral properties of the data collected by ASTER have been used for example in detecting changes on forested surfaces within a model area in the Russian Federation (Raši & Hlásny 2005). These data are also used within the international aid projects in developing countries by the Czech Geological Service (Kopačková 2004). In extreme weather conditions as seen in regions with minimal vegetation cover, severe erosion and volcanic activities such as Mongolia, El Salvador, Peru and the Antarctic, the use of RS is also largely implemented. For example, in Mongolia the project is focused on land mapping for mining prospects. The data collected by ASTER are also utilised within the project on mineralogical mapping and the so called hyperspectral data analysis. In Turkmenistan, spectral analysis was made on the basis of the data collected by ASTER for mapping groups of minerals. The high occurrence of geological events, volcanoes, and hydrothermal sediments of Zn and Pb can offer valuable information for understanding the sedimentology of the South Caspian basin (Junek 2003).

Data

For the purposes of this work, L1B data acquired by ASTER were used (Table 1). The advance of this type of data is that the radiometric and geometric coefficients have already been applied.

Four scenes covering two adjoining areas in north-south direction west of Prague were selected from the available set of 13 scenes provided for the Project VaV-SM 10/70/04. The scenes dated from May 2002 and July 2005 cover almost the same area. The cloud cover does not exceed 15% of the scene. The size of the area of interest is about 60 × 120 km. The area of approximately rectangular shape is bordered by the following towns: Pirna (Germany), Hrádek nad Nisou, Slapy, Kladruby (Figure 1).

The area depicted in the satellite images has a rather rugged topography. On a territory of approx. 6000 km^2 is situated the Elbe River Lowland (with the lowest point of the area of interest – on the Elbe river, 115 m above sea level), the Czech table, the Central Bohemia Upland, the Brdy Upland, and the Czech Central Mountains, the Krušné

Table 1. ASTER L1B data description (Registered Radiance at the Sensor) (Anonym 2006a)

Size of scan area	~60 km × 60 km
Image size	VNIR (1, 2, 3N): 4200 raws × 4980 columns VNIR (3B): 4600 raws × 4980 columns SWIR: 2100 raws × 2490 columns TIR: 700 raws × 830 columns
File size	VNIR (1, 2, 3N) = ~60 MB VNIR (3B) = ~22 MB SWIR (4–9) = ~30 MB TIR (10–14) = ~6 MB Total = 118 MB
Spatial resolution	VNIR = 15 m SWIR = 30 m TIR = 90 m
Data format:	Hierarchical Data Format-Earth Observing System (HDF-EOS)
Projection	Universal Transverse Mercator (UTM)

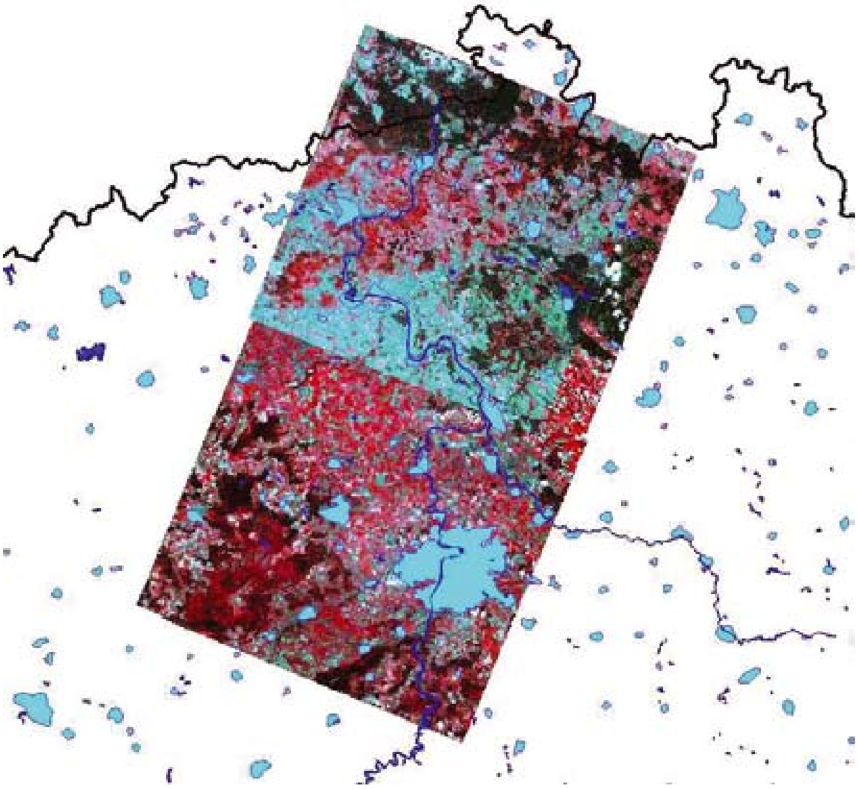

Figure 1. Area of interest

Mountains, and the adjoining Lužické Mountains (with the highest point of the area – Luž Mountain 793 m a.s.l.).

Working process

The data acquired by the VNIR subsystem can be stereoscopically evaluated. Using the principles of spectroscopy, it is possible to generate DSM from 3N and 3B images. DSM can be subsequently used for the creation of orthophoto, where the 3N scene or other multispectral channels are used for colour composite.

The resultant model and orthophoto are transformed to a reference co-ordinate system using the control points, i.e. the points with known X, Y, Z co-ordinates. Regarding the extent of the area (approx. 6000 km^2) and resolution (15 m/px), the co-ordinates of the control points were determined using a map in the scale of 1:10 000 with basic contour interval 2 m (5 m at times).

Digital surface model

At first, the database of the control points was created. For each scene 21 points were determined. The database contains 84 points in total. X and Y co-ordinates of these points are determined in S-42 co-ordinate system, Z co-ordinate is in the Baltic Vertical Datum (after adjustment). Several facts played an important role during the selection of the points: uniform distribution of points in the scene, points not covered with clouds, easy identification of points in both images (3N and 3B) and on the map. A more complicated task was the determination of the elevation of the control points using the map; e.g. crossroads are often chosen as unambiguously identifiable points but it is usually difficult to determine the elevation of flyover junctions.

As accuracy specification of image matching, a root mean square error (RMS) was chosen. RMS of image matching ranges from 9.6 to 13.7 m. The maximum difference of RMS within the stereo-pair is 2.6 m only.

3B and 3N scenes do not represent a typical photogrammetric stereo-pair. Before the stereoscopic determination of the elevation, it is necessary to convert the original data to epipolar pairs.

After the selection of the control points on scenes, epipolar pairs were generated. Using the epipolar pairs, DSM can be subsequently calculated based on the image correlation.

There are several parameters which influence the result of DSM calculation. The DSM created is always related to the highest points of the area, i.e. tree tops, housetops, etc.

During DSM creation, various parameters were tested and in the end two models were created. These models differ especially in resolution.

The resolution of the first model (called H1) is 15 m/px, the resolution of the second model (called H2) is 30 m/px. For 4 scenes, 8 DSM were generated in total, i.e. H1 and H2 models for each scene. H1 and H2 models were compared using four methods:

(1) Comparison of the following accuracy specifications calculated within DSM generation: the elevation standard error, arithmetic mean value of differences in elevation, maximum absolute value of the difference in elevation. The statistical evaluation shows that the values of accuracy specifications of both models highly resemble. The elevation standard error of the control points is about 30 m.

(2) Visual method. In the comparison of the models, emphasis was placed on the method of terrain representation, interpretability of the terrain, and filtration method of the cloud cover and noise. H2 models show a reduced sharpness of edges, colour transitions are smoother in the monochromatic image, and the models are better interpretable (Figure 2). On the contrary, it is possible to recognise details in H1, such as highways.

(3) Next test was aimed at the comparison of the created DSM and the map base, as a representative source of terrain information. 24 checkpoints were selected in the area of interest and the area was divided into the northern (N) and the southern (S) parts. In each part, 12 points with a uniform distribution were chosen. The following accuracy specifications were determined for the checkpoints: RMS, RMSx, RMSy, RMSz (Table 2). The comparison of the accuracy specifications shows that the position accuracy of the models is up to 15 m, i.e. similar to the position accuracy of the control points. RMSz of H1 and H2 models, calculated from the data acquired in 2002 in the northern part of the area, does not exceed 20 m, RMSz of other models ranges from 35 m to 39 m. A model having RMSz about 20 m was created for the image with the lowest (almost none) cloud cover. The cloud cover of models with the highest RMSz is approx. 10% of the scene. We can say that the accuracy of H1 and H2 models is almost the same.

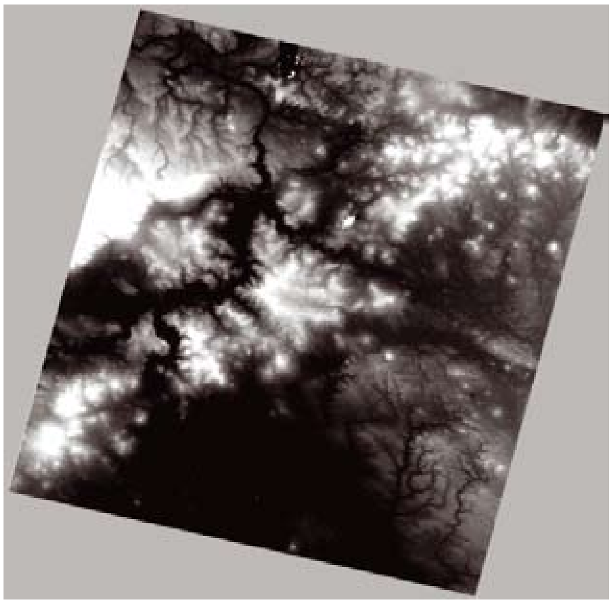

Figure 2. DSM of the northern part of the area of interest; data were acquired in 2002

RMS – mean co-ordinate error,

$$RMS = \sqrt{\left(\frac{\left[(x-x')^2+(y-y')^2\right]}{n}\right)}$$

Table 2. Accuracy specifications of DSM check points (in m)

Model	DSM H1				DSM H2			
	RMS	RMSx	RMSy	RMSz	RMS	RMSx	RMSy	RMSz
N 2005	12.2	11.5	3.9	36.8	13.9	13.0	5.2	38.6
S 2005	11.1	7.6	8.0	36.0	12.1	7.7	9.4	35.6
N 2002	13.1	10.0	8.6	20.0	14.6	9.9	10.8	19.7
S 2002	14.1	7.5	12.0	38.4	13.9	6.6	12.2	38.5

RMSx – mean error of co-ordinate x,

$$RMSx = \sqrt{\left(\frac{[(x-x')^2]}{n}\right)}$$

RMSy – mean error of co-ordinate y,

$$RMSy = \sqrt{\left(\frac{[(y-y')^2]}{n}\right)}$$

RMSz – mean error of co-ordinate z,

$$RMSz = \sqrt{\left(\frac{[(z-z')^2]}{n}\right)}$$

where:
y – map co-ordinate y
x – map co-ordinate x
z – map elevation
y′ – calculated coordinate y
x′ – calculated coordinate x
z′ – calculated elevation
n – number of points

The final test compared the differences in elevation of two corresponding model cut-outs from different years. The comparison was made of the cut-outs of two models calculated with the use of the same parameters, the size of the cut-out being 7500 × 7500 m. The comparison consisted in subtraction of the models elevations according the following formula: $\Delta Z = Z_{2002} - Z_{2005}$. Whereas in the first case the mean error of random samplings is meant, in the case of cut-outs the standard mean error could be calculated.

RMSZ – mean error of elevation difference,

$$RMSZ = \sqrt{\left(\frac{[(z-z')^2]}{n}\right)}$$

AVGZ – average value of elevation difference,

$$ACGZ = \frac{[(z-z')]}{n}$$

AVG|Z| – average of absolute value of elevation difference,

$$AVG|Z| = \frac{[|(z-z')|]}{n}$$

Max |Z| – maximum absolute value of elevation difference

where:
z – elevation in 1st model elevation
z′ – elevation in 2nd model elevation
n – number of points

An area situated east of Ústí nad Labem in the northern part and an area near Kladno situated in the southern part (Figure 3) were selected for the comparison of DSM cut-outs. The northern area is a mid-mountain terrain, the southern part is a slightly undulating terrain.

The comparison was made between models of the same area but coming from different years, the southern cut-out giving better results. The standard error in the difference of elevations between the models of the northern part is about 40 m (Table 3). The difference in the determination of the model accuracy is also visible on the comparison of the outputs (Figures 4–6), there is evidently a correlation between the elevation and the accuracy of DSM .

The same comparison was applied to the whole set of DSM H2. The areas which were described as an error during the calculation (areas covered with clouds) were excluded from the calculation of the models.

Besides the basic accuracy specifications of the whole set, a calculation was made for a set with a limited maximum difference in elevation. The limit

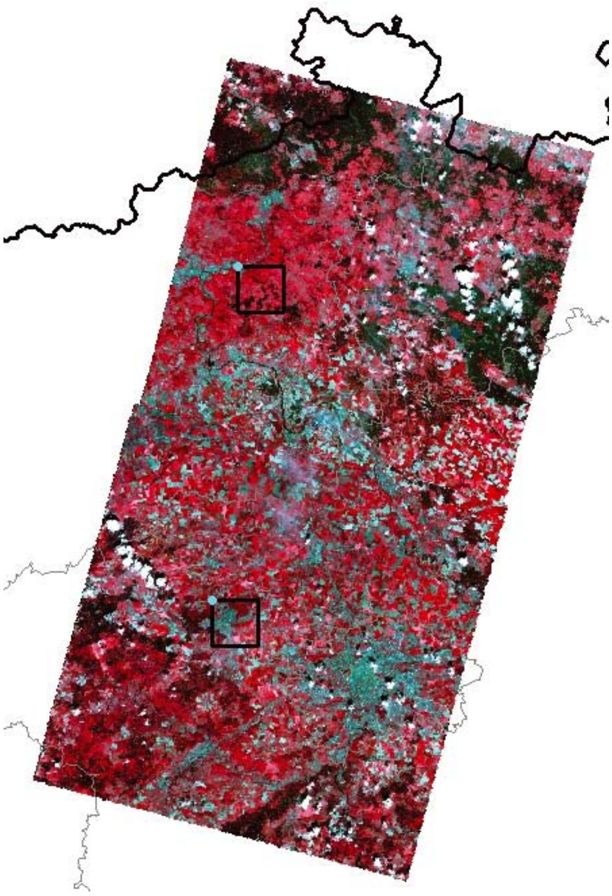

Figure 3. Location of the cut-outs in the area of interest

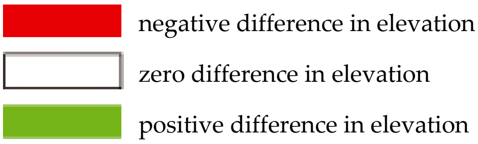

Figure 4. Key of the comparison of cut-outs

was up to 60 m, i.e. up to the doubled elevation standard error of the control points, and 80 m.

The comparison of the models shows that the models of the northern and the southern regions have been created with almost the same RMSz (52 m, Table 4). In addition to this, both comparisons of the models show that the models from different years are very similar in the elevation of 350 m (Figures 7–9). The selected regions represent a heterogeneous terrain, there are agricultural areas of the Central Bohemia as well as wooded hillsides of the border mountains. We can assume that the error between the models (52 m) from both years is caused by different conditions during the data acquisition.

Each compared point was determined from a different angle because the positions of the centre of the scanner were different in the years 2002 and 2005 (about 10 km in the east-west direction).

Orthophoto

A photograph is generally a central projection of the scan area; a radial distortion affects the position of points placed on it. This is the reason why it is not possible to use the photograph directly for the creation of a map or as a GIS layer.

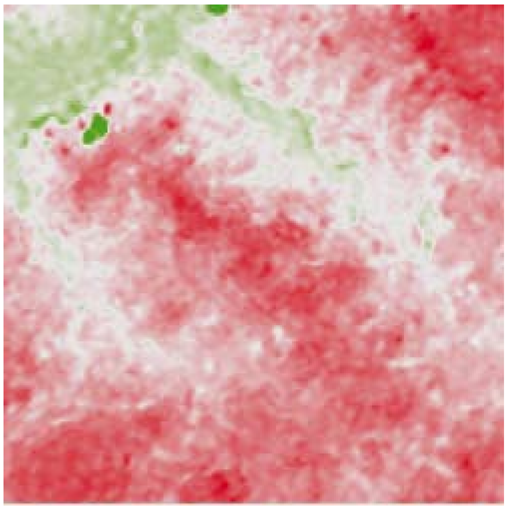

Figure 5. Representation of comparison of cut-outs of the northern part of the area

The creation of an orthophoto consists in the conversion of the original data with radial distortion to an orthogonal projection. A colour orthophoto is created from ASTER RGB data (channels 1, 2, 3N) and DSM (a source of information about the elevation for each pixel of the newly created orthophoto, Figure 10). The pixel size of the resultant orthophoto is 15 × 15 m, regardless which DSM type (H1 and H2) was chosen as the source of information about

Table 3. Accuracy specifications of the comparison of two DSM cut-outs (in m)

Comparison of cut-outs	DSM H1				DSM H2			
	RMSZ	AVGZ	AVG |Z|	Max |Z|	RMSZ	AVGZ	AVG |Z|	Max |Z|
Northern area	40.7	28.8	34.9	293.9	39.9	28.3	34.2	293,5
Southern area	16.8	5.7	12.2	259.9	14.9	5.3	10.8	262,9

Table 4. Accuracy specifications of comparison between two DSM

Comparison of models	Northern area					Southern area				
	whole set (%)	RMSZ (m)	AVGZ (m)	AVG |Z| (m)	Max |Z| (m)	whole set (%)	RMSZ (m)	AVGZ (m)	AVG |Z| (m)	Max |Z| (m)
ΔZ ≤ 60 m	93.49	26.12	4.53	21.56	60.00	92.07	29.70	12.56	24.98	60.00
ΔZ ≤ 80 m	97.07	28.78	3.56	23.27	80.00	97.30	32.69	14.62	27.18	80.00
Whole set	100.00	52.63	0.00	28.24	1138.62	100.00	52.44	14.68	32.18	827.34

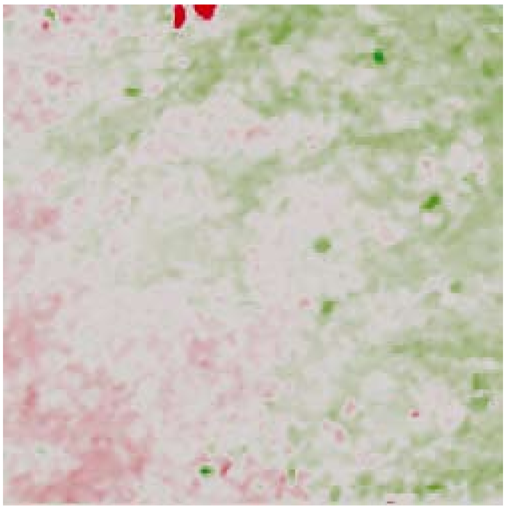

Figure 6. Representation of comparison of cut-outs of the southern part of the area (in the east-west direction)

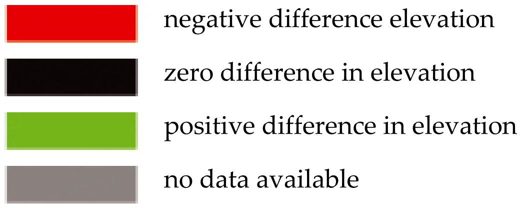

Figure 7. Key of the comparison of models

the elevation, and corresponds to the geometric resolution of the original data.

For the accuracy assessment, 26 checkpoints were selected in the area of interest. The area was divided into the northern (N) and the southern (S) parts again, 13 points with a uniform distribution in the orthophoto were selected in each part. The

Table 5. Accuracy specifications of check points (in m)

Ortophoto	O H1			O H2		
	RMS	RMSx	RMSy	RMS	RMSx	RMSy
N 2005	12.4	11.8	3.9	14.0	12.9	5.24
S 2005	11.6	8.2	8.2	12.5	8.2	9.5
N 2002	13.2	10.0	8.6	14.8	10.1	10.8
S 2002	14.4	7.8	12.1	14.9	6.6	13.3

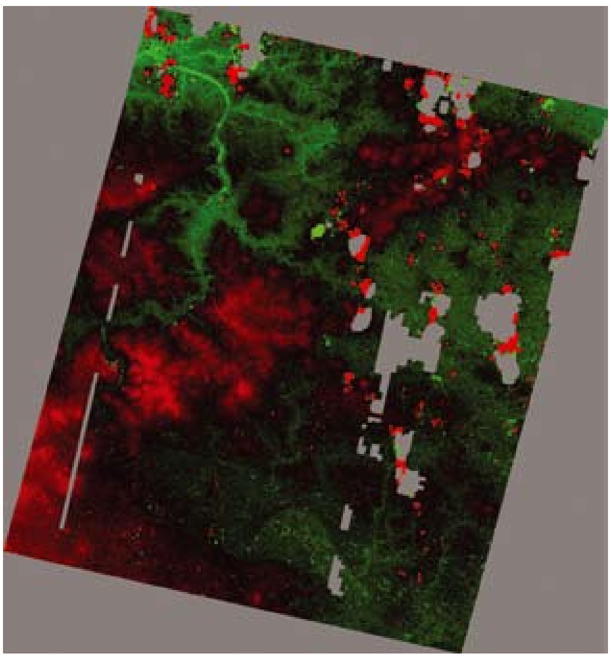

Figure 8. Representation of comparison of the northern part of the area

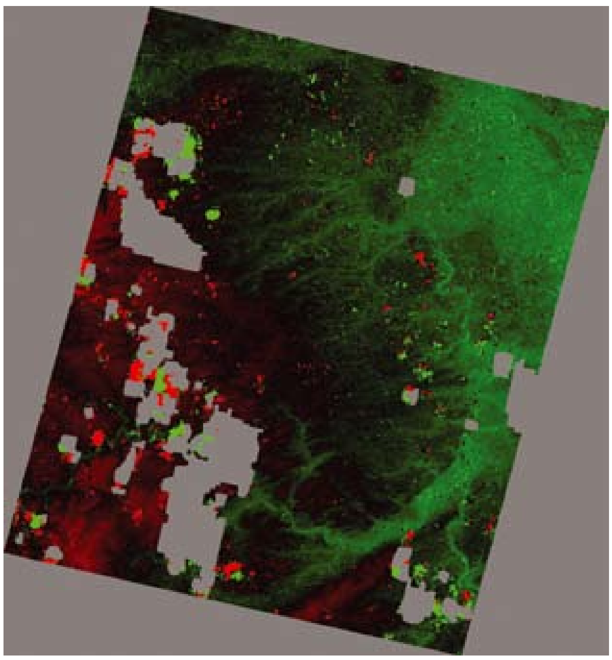

Figure 9. Representation of comparison of the southern part of the area

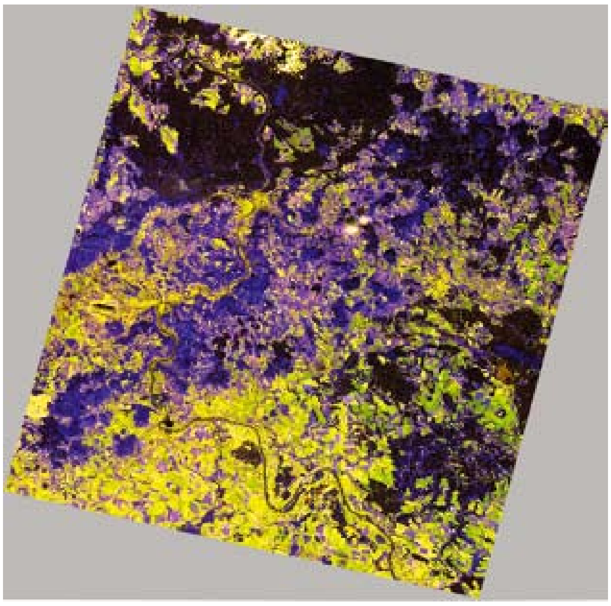

Figure 10. Orthophoto of the northern part of the area of interest; data were acquired in 2002

following accuracy specifications of the checkpoints were determined (Table 5): RMS, RMSx, and RMSy.

The table shows that the RMS of no orthophoto exceeds 15 m. In addition to that, RMS of the checkpoints has a low variance.

CONCLUSION AND DISCUSSION

The position accuracy of the digital surface models created is similar in all of them (up to 15 m), i.e. approx. 1 pixel. But the elevation accuracy varies. The elevation standard error of the model of the northern part of the area coming from 2002 does not exceed 20 m, the elevation standard error of other models is 35 m. Nevertheless, the elevation standard error of the control points listed in the computation protocol is about 30 m with all models. The comparison of H1 and H2 models shows that the same accuracy has been achieved for both of them. The visual method shows that H2 model is more suitable for the elevation representation, especially as concerns the interpretability of the terrain.

When performing the assessment of the elevation accuracy of the model created, it is necessary to realise that the elevations of the control and checkpoints were determined using a contour plan showing the land surface without buildings and vegetation. However, the DSM calculation involves the surface as a whole. The comparison of the accuracy specifications does not directly show the factors of the resultant model.

We can assume that the cloud cover, terrain configuration, and viewing angle affect the accuracy.

The comparison of the models coming from years 2002 and 2005 and representing the same area showed that the models highly resembled in the elevation of about 350 m. Total standard error of the models was 52 m.

The tests performed on a set of 13 check points of orthophoto proved that, by using DSM with RMS up to 15 m and RMSz up to 40 m, it is possible to create orthophoto with RMSx,y up to 15 m, i.e. up to the spatial resolution of the processed data.

The results show that the created orthophoto can be used as a basis for the creation of small-scale maps, but only exceptionally as a basis for the creation of medium-scale maps.

Ortophotos together with DSM (digital surface models) can become part of the information systems which are presently used in several domains. Ortophotos and DSM may be a supporting surface for the visualisation of study outcomes when bare facts are presented to specialised or lay public. These data may be used in practical landscape management in the fields of water management, agriculture, or forestry.

Further utilisation of RS is also possible in pedology. Basic characteristics, such as the type of the vegetation cover, ground characteristics, surface materials, surface runoff or soil patterns may be used in forecasting models. During spectral analysis of the data supplied by the ASTER scanner, the hypespectral classification method may be applied on the basis of spectral curves of specific types of soils and minerals (spectral soil library). Such analysis enables a comprehensive classification of soil types, which is useful particularly in arid regions. In the Czech Republic, this classification can be used in the North Bohemian brown coal basin or in agricultural regions in early springs or in autumns, when large land surfaces are without vegetation. Forested areas or areas with vegetation propagation are not appropriate sites in our regions for this type of research.

References

Anonym (2006a). Land Processes Distributed Active Archive Centre. (online) Available at http://edcdaac.usgs.gov/aster/ast_l1b.asp. (accessed October 19, 2006)

Anonym (2006b): Terra (formerly EOS AM-1). (online) Available at http://science.hq.nasa.gov/missions/satellite_52.htm. (accessed May 2, 2006)

Anonym (2006c): Velká encyklopedie družic a kosmických sond. (online) Available at http://www.lib.cas.cz/www/space.40/INDEX1.HTM. (accessed May 2, 2006)

Junek P. (2003): Geological Mapping in the Cheleken Peninsula, Turkmenistan area using Advanced Spaceborne Thermal Emission and Reflection Radiometer (ASTER) Data. Delft University of Technology. Faculty of Civil Engineering and Geosciences. Department of Applied Earth Sciences. Delft.

Kopačková V. (2004): Využití metod dálkového průzkumu Země v České geologické službě. (online). Available at http://www.arcdata.cz/download/ArcRevue/2004/4/24-vyuziti-DPZ-v-CGS-4-2004.pdf (accessed May 2, 2006)

Raši R., Hlásny T. (2006): Satelitný skener Aster a jeho využitie pre detekci zmien v pokrývke lesa na príklade modelových území z dalekého východu. Zborník príspevkov GIS 2005. (online) Technická univerzita vo Zvolene, Lesnícka fakulta, Katedra hospodárskej úpravy lesov a geodézie, Zvolen, 115–123. Available at http://www.sagi.sk/Portals/0/zbornik_gis_2005.pdf (accessed Septembetr 10, 2006)

Received for publication April 19, 2007
Accepted after corrections, February 2, 2008

Corresponding author:

Ing. Dana Tollingerová, Ph.D., Česká zemědělská univerzite v Praze, Fakulta životního prostředí,
Kamýcká 129, 165 21 Praha 6-Suchdol
tel.: + 420 224 382 159, e-mail: tollingerová@fzp.czu.cz